

# AIR-REACTIVITY OF CHARs FROM LDPE PYROLYSIS

Noelia Alonso-Morales, Miguel A. Gilarranz, Francisco Heras, Valentin González, Juan J. Rodríguez  
Sección Departamental de Ingeniería Química, Facultad de Ciencias. Universidad Autónoma de Madrid,  
Carretera de Colmenar km 15, 28049 Madrid, Spain  
Email: [miguel.gilarranz@uam.es](mailto:miguel.gilarranz@uam.es)

## Introduction

LDPE is the most extensively used plastic and it highly contributes to the plastic wastes pool. As a result of this, the investigation of routes of valorisation for LDPE wastes is an important environmental concern. Pyrolysis has been widely studied as an interesting way of valorisation and much information about this topic can be found in the literature (Poustma et al, 2003; Hernandez et al, 2006). Nevertheless, most of the works are focussed on gas and condensable fraction since in general low yields of char have been reported (Cozzani et al, 1997). Pyrolytic char from LDPE can be a potential precursor for carbon materials and this is an investigation addressed to explore the properties of those chars.

The pyrolysis of LDPE to maximize the production of char was studied in a previous work (Alonso-Morales et al, 2006), where high char yields, between 27% and 49%, were obtained. The yield was found to be dependent on the pyrolysis temperature, the nitrogen flow rate through the reactor and LDPE feed rate. The study of the microstructure and morphology of the chars revealed that they consist of clustered nanospheres (Figure 1). The pyrolysis conditions also showed a significant influence on the size of the nanospheres. Thus, Figure 1 shows how the size of the nanospheres can be controlled by the means of the pyrolysis temperature.

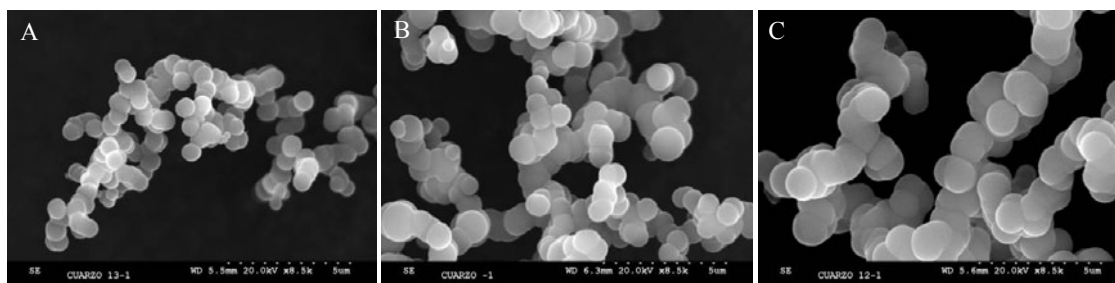


**Figure 1.** SEM images of char obtained at different pyrolysis temperature (A 776 °C; B 860 °C and C 944 °C).

The study of the reactivity is a very interesting approach to the characteristics of the chars. Besides, this study can provide important information for the development of gasification processes if the preparation or activated carbon is intended (Encinar et al, 2000). The reactivity of the chars depends on a number of factors including carbon structure, diffusion of reactants, changes in surface reactivity during the reactions, temperature, etc. (Jin et al, 2005), and the reactivity studies can be performed by different methods. Thermogravimetric analysis (TGA) combined to differential thermogravimetric analysis (DTG) are extensively used to study the reactivity of carbon samples. These techniques can show differences in reactivity for chars with different characteristics (De la Puente et al, 2000). In this work the air reactivity of chars obtained from LDPE under different pyrolysis conditions was evaluated by TGA and DTG.

## Materials and Methods

Low density polyethylene (LDPE) from Dow Chemical was used. LDPE virgin pellets were grinded in blade mill (IKA Labortechnik) using liquid nitrogen as cooling agent. After grinding the fraction with a particle size between 2.0 and 2.8 mm was separated for the pyrolysis runs. The pyrolysis experiments were carried out by semicontinuous operation in a vertical furnace. The temperature was controlled by means of two electrical heaters, one in the reaction zone and another at the gas inlet. LDPE was fed continuously into the reactor from a loader by means of a solids valve. An amount of about 0.05 g of LDPE was feed in each discharge. The time between discharges allowed controlling the LDPE feed rate. Nitrogen was fed along the experiment from the lower part of the furnace after preheating. More information about the experimental setup can be found in a previous work (Alonso-Morales et al, 2006).

The air reactivity of the chars was studied in the thermo gravimetric system described in Figure 2 (CI Instruments). The temperature is controlled by means of an electrical heater. The char is placed in the pan carrier. An amount of 10 mg of sample is used in each experiment. The pan carrier is connected with the head of the balance by rods. The pan carrier and rods are inside the quartz universal attachment which closes the system to keep gaseous atmosphere. Air is used as reactive gas. The head of the balance detected the mass changes when the air reacts with the char sample. The runs were performed from 20 °C to 900 °C at a heating rate of 10 °C/min. An air flow of 60 NmL/min was maintained by means of a mass flow controller.

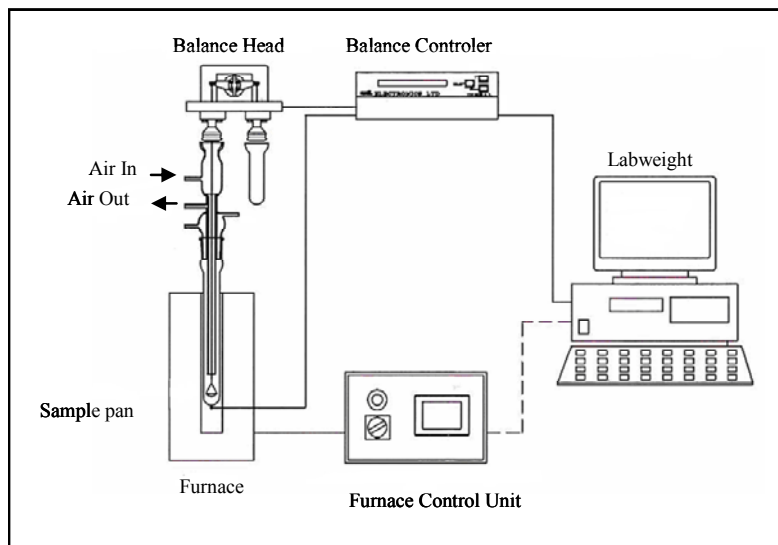


**Figure 2.** Schematic diagram of the microbalance reaction system.

DTG curves were calculated from TGA data. Char reactivity is defined as the weight loss rate calculated from the weight loss curves as:

$$(r) = \frac{1}{m_0} \frac{-dm}{dt} = \frac{dX}{dt} \quad [\text{Eq. 1}]$$

where  $m_0$  is the initial mass of char,  $m$  is the mass of carbon sample,  $t$  is the reaction time and  $X$  is the char conversion, defined as:

$$X = \frac{m_0 - m}{m_0} \quad [\text{Eq. 2}]$$

Activation energies were calculated from pairs of weight loss/temperatures values provided by the thermogravimetric analyser, using the kinetic equation:

$$\ln\left(\frac{1}{1-X} \frac{dX}{dt}\right) = \ln A - \frac{E_a}{RT} \quad [\text{Eq. 3}]$$

where  $E_a$  is the activation energy and  $A$  the Arrhenius factor.

### **Statistical approach**

The influence of the pyrolysis conditions on the air reactivity of the char was studied by means of a response surface method. The variables considered were pyrolysis temperature ( $T$ , 776-944°C), nitrogen flow through the pyrolysis reactor ( $F$ , 0-50 NmL/min) and time between the LDPE discharges to the pyrolysis reactor

(t, 16-109 s). The responses considered were the parameters obtained from the thermogravimetric analysis of the chars. The maximum reactivity temperature ( $T_{max}$ ) was identified from the peak in DTG plot. The Arrhenius plots obtained from TGA data showed two different slopes for all the char samples analyzed. From these plots the activation energy at low temperature ( $E_{a_{low}}$ ), the activation energy at high temperature ( $E_{a_{high}}$ ) and the transition temperature ( $T_{trans}$ ) were calculated. Figure 3 shows the TGA, DTG and Arrhenius plot for char sample number 10, which is representative of the results obtained for the rest of the samples.

The experimental design applied was a  $2^3$  central composite design, which includes three main effects, three two-factor interactions and one three factor interaction. The experimental matrix is shown in Table 1. The low and high levels of the variables are denoted by “-1” and “+1”, respectively. The position of the  $2^3$  factorial points and the central points are represented by  $(\pm 1, \pm 1, \pm 1)$  and  $(0, 0, 0)$ , respectively. The axial points are placed at  $(\pm 1.68, 0, 0)$ ,  $(0, \pm 1.68, 0)$  and  $(0, 0, \pm 1.68)$ . This axial distance corresponds to a rotatable design. To correlate the experimental results quadratic equations were employed. The analysis of variance (ANOVA) for experimental results was used to identify non-significant effects, which were excluded from the model regression, and to check the suitability of the model. The software package *Statgraphics 5.0* was used to carry out ANOVA and model regressions. Contour maps (two dimensional of response surfaces) from models were employed analyze the influence of the variables. Details about response surface methods can be found elsewhere (Montgomery, 1991).

**Table 1.** Experimental matrix and parameters calculated by thermogravimetric analysis of the chars obtained at different pyrolysis conditions.

Char sample	Pyrolysis conditions			TGA and DTG parameters			
	T (°C)	F (Nml/min)	t (s)	$T_{max}$ (°C)	$T_{trans}$ (°C)	$E_{a_{low}}$ (kJ/mol)	$E_{a_{high}}$ (kJ/mol)
1	910	40	90	759	736	156	66
2	910	10	90	772	738	201	48
3	910	40	35	704	660	186	96
4	910	10	35	737	711	171	56
5	810	40	90	606	552	270	68
6	810	10	90	731	720	132	69
7	810	40	35	666	553	269	93
8	810	10	35	655	638	206	80
9	860	25	63	629	538	246	92
10	860	25	63	629	551	264	93
11	944	25	63	671	560	248	80
12	776	25	63	628	540	215	115
13	860	25	109	756	706	241	114
14	860	25	16	623	563	263	91
15	860	50	63	632	553	246	95
16	860	0	63	739	717	165	97

## Results and discussion

Table 2 shows the results obtained from the ANOVA applied to the TGA and DTG parameters summarized in Table 1. From the F distribution values the effects with a significance level lower than 85% ( $F < 16.8$ ) were neglected for models regression. The ANOVA indicates that it was not possible to obtain a suitable model for  $E_{a_{high}}$ , since the model only accounted for 35.0% of the total variability. To correlate the experimental results quadratic equations were developed. The ANOVA for the final models showed that the sum of squares of the models for the responses  $T_{max}$  and  $T_{trans}$  accounted for 76.2 and 81.5% of the total variability, respectively, which can be considered as acceptable for the description of the influence of the variables. In the case of  $E_{a_{low}}$  the effect of temperature (T) was included to obtain a hierarchical model, since the interaction of temperature and nitrogen flow (TF) was significant. However, the model for  $E_{a_{low}}$  accounted for 60.3% of the total variability, a rather low value that indicate that only general information about the trends can be obtained from the model. The models developed were the following:

$$T_{\max} (^{\circ}\text{C}) = 3720.7 - 7.442 T - 2.505 t - 4.877 F - 0.0352 Tt + 0.00466 T^2 + 0.0341 t^2 + 0.108 C^2$$

$$T_{\text{trans}} (^{\circ}\text{C}) = 5328.78 - 10.095 T - 6.179 t - 41.373 F + 0.0333 TF + 0.00574 T^2 + 0.0585 t^2 + 0.197 F^2$$

$$Ea_{\text{low}} (\text{kJ/mol}) = -546.09 + 0.805 T + 38.499 F - 0.0385 TF - 0.0778 F^2$$

**Table 2.** ANOVA for experimental results in Table 1.

Source of variance <sup>a</sup>	$T_{\max}$		$T_{\text{trans}}$		$Ea_{\text{low}}$		$Ea_{\text{high}}$	
	Sum of squares	$F$	Sum of squares	$F$	Sum of squares	$F$	Sum of squares	$F$
t	7958.49	159.2	13194.6	156.2	885.99	5.5	91.3	182.7
T	10927.49	218.6	12649.5	149.7	846.19	5.2	774.8	1549.5
F	8462.22	169.2	24786.6	293.3	6911.35	42.7	325.1	650.3
tT	684.50	13.7	60.5	0.72	666.13	4.1	0.5	1.0
tF	1682.00	33.6	144.5	1.71	28.13	0.2	162.0	324.0
TF	578.00	11.6	5000.0	59.2	6670.13	41.2	264.5	529.0
$t^2$	6157.56	123.2	18116.3	214.4	574.58	3.6	70.7	141.5
$T^2$	1254.97	25.1	1906.6	22.6	2118.80	13.1	190.2	380.4
$C^2$	5500.55	110.0	18261.5	216.1	5477.41	33.8	237.3	474.7
Lack-of-fit	10339.82	41.4	18613.7	44.1	8066.68	10.0	712.2	1424.4
Pure error	50.00		84.5		162.00		0.5	
Total	49024.44		101885.0		30161.94		5481.9	

<sup>a</sup>: degrees of freedom for effects, lack-of-fit, pure error and model total sum of squares are 1, 5, 1 and 15, respectively

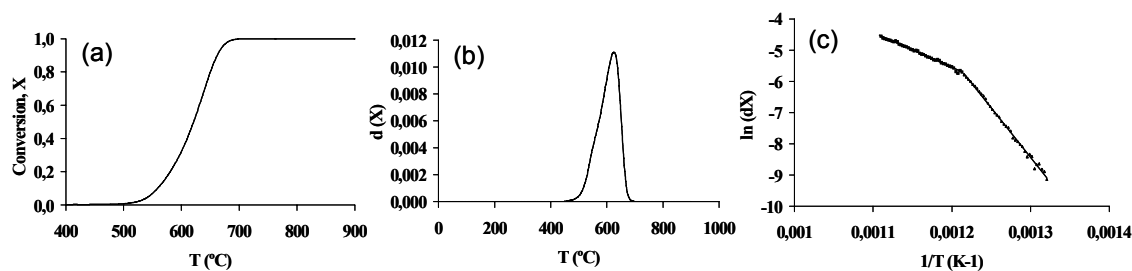


**Figure 3.** TGA (a), DTG (b) and Arrhenius (c) plots for char sample number 10.

Figure 4 shows the contour plots for  $T_{\max}$  for a constant nitrogen flow of 25 NmL/min. From this figure it can be seen that  $T_{\max}$  increases with the pyrolysis temperature. This trend is in agreement with the more ordered structure, and hence lower reactivity, of the chars treated at high temperature (Rodriguez-Mirasol et al, 1997).  $T_{\max}$  also increases with the time between the LPDE discharges to the pyrolysis reactor. A higher time between discharges reduces the amount of gases generated by pyrolysis. Therefore the self displacement of the gases decreases and a higher residence time in the pyrolysis reactor is achieved. Under these conditions secondary and tertiary gas phase reactions take place in higher extension, which can lead to a higher proportion of olefins and other low molecular weight species that are precursors of more ordered pyrolytic carbon (Cozzani et al, 1997).

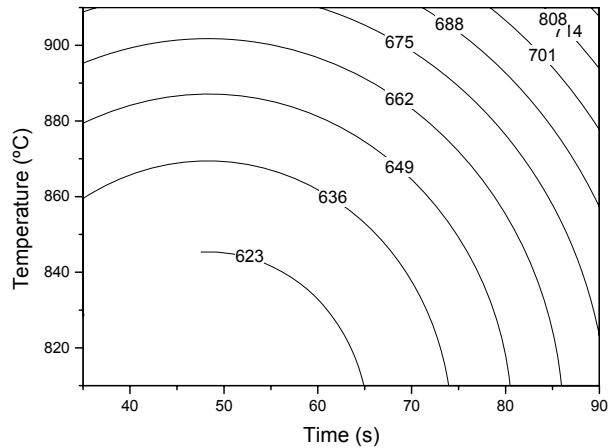


**Figure 4.** Contour plot for  $T_{\max}$  ( $F = 25$  NmL/min).

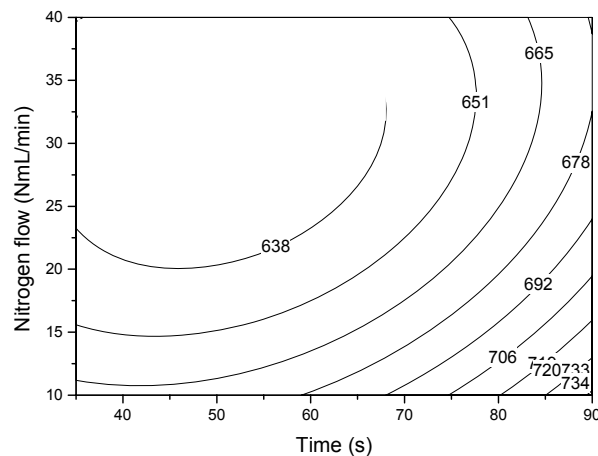


**Figure 5.** Contour plot for  $T_{\max}$  ( $T = 860^{\circ}\text{C}$ ).

The influence of nitrogen flow rate can be observed in Figure 5. The use of high nitrogen flow rates produces a displacement of the pyrolysis products and reduces their residence time in the reactor. The result is the deposition of pyrolytic carbon as a more reactive structure. The significance of the quadratic effects shown in Table 2 is also reflected in Figures 4 and 5. Thus, the slope of the surface becomes higher as the temperature and the time increase, and as the flow decreases. Likewise, Table 2 shows that there is a significant interaction between time and flow ( $tC$ ). The combination of long times between discharges and high nitrogen flows leads to a decrease in  $T_{\max}$ , probably due to a dilution of pyrolysis products, which can be a drawback for pyrolytic carbon deposition. The combination of high temperatures, long times between discharges and low nitrogen flow rates would be advisable in order to obtain chars for application where a low reactivity is desired, or if a further graphitization by thermal treatment is intended.

The contour plots for the transition temperature ( $T_{\text{trans}}$ ) in the Arrhenius plots can be seen in Figures 6 and 7. The influence of the pyrolysis conditions on the  $T_{\text{trans}}$  of the chars is similar to that found for  $T_{\max}$ . It can be seen that  $T_{\text{trans}}$  increases with the pyrolysis temperature and the time between discharges, and that it decreases with nitrogen flow rate. Therefore, for those chars whose structure is more ordered and less reactive the chemical reaction is slower and it remains as the controlling step up to higher temperatures.

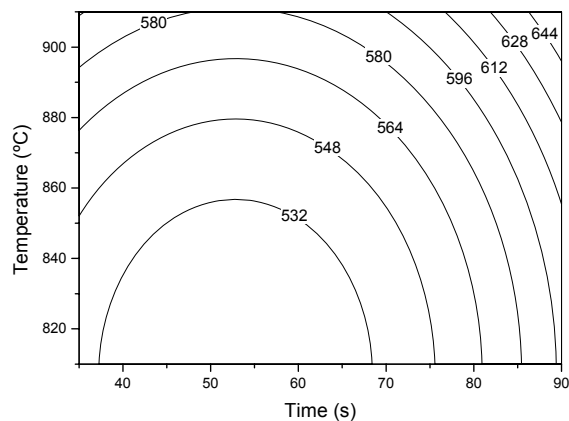


**Figure 6.** Contour plot for  $T_{trans}$  ( $F = 25 \text{ NmL/min}$ ).

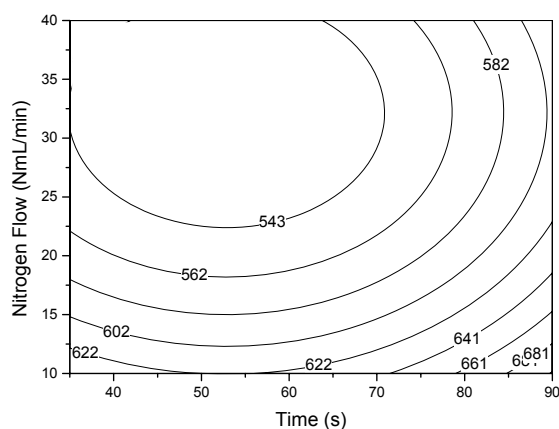


**Figure 7.** Contour plot for  $T_{trans}$  ( $T = 860^\circ\text{C}$ ).

As it was indicated above, the model developed for  $E_{a_{low}}$  did not provided a suitable contour map to study the influence of the pyrolysis variables. However, some trends can be observed when  $E_{a_{low}}$  is plotted *versus*  $T_{max}$ , as it can be seen in Figure 8. In general, the char samples that exhibited a higher  $T_{max}$  value also showed a lower activation energy in the low temperature range. Those chars with lower reactivity ( $T_{max} > 700^\circ\text{C}$ ) showed in general  $E_{a_{low}}$  values well below 200 kJ/mol. Such low values could indicate combined chemical and physical control, although they can also indicate that the chars have an heterogeneous structure and that a fraction of them has a lower reactivity. With regard to  $E_{a_{high}}$ , no trend was observed for the data obtained. The values of  $E_{a_{high}}$ , for the set of char samples studied indicate that at high temperatures the reaction is clearly controlled by physical mechanisms.

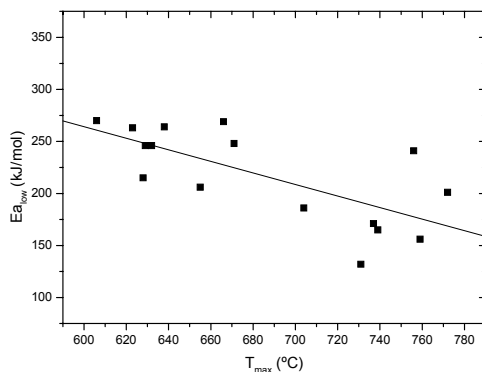


**Figure 8.**  $E_{a_{low}}$  vs  $T_{max}$  for the char samples studied.

## Conclusions

The influence of pyrolysis conditions of LDPE on the char structure can be study by means of reactivity analysis. Statistical approach can be used to employ a response surface method.

The values of temperature of maximum char reactivity ( $T_{max}$ ) show that less reactive carbons are obtained at higher temperatures, lower nitrogen flow rate and lower LDPE feed rate during pyrolysis process. The less reactivity indicates that more ordered carbons can be obtained under these conditions.

Arrhenius plot shows two different slopes for all the samples which indicate a change in the mechanism of reaction, controlled by physical mechanisms at high temperatures. In general, the char samples that exhibited a higher  $T_{max}$  value also showed lower activation energy in the low temperature range ( $E_{a,low}$ ).

## Acknowledgement

The authors are grateful to the Spanish Ministry of Education and Science for financial support (project CTQ2006-13512). Noelia Alonso-Morales would like to thank to the Spanish Ministerio de Educacion y Ciencia for the FPI Research Fellowship BES-2004-4060.

## References

- Alonso-Morales, N. Gilarranz, M.A. Heras, F. González, V. Rodríguez, J.J. 2006. Study of the conversion of low density polyethylene to solid carbon materials by pyrolysis. The International Carbon Conference, Aberdeen, Scotland (16<sup>th</sup>-21<sup>st</sup> July).
- Cozzani, V. Nicoletta, C. Rovatti, M. and Tognotti, L. 1997. Influence of Gas-Phase Reactions on the product yields obtained in the pyrolysis of polyethylene. *Industrial & engineering chemistry research*, 36: 342-348.
- De la Puente, G. Fuente E. Pis J.J. 2000. Reactivity of pyrolysis chars related to precursor coal chemistry. *Journal of Analytical and Applied Pyrolysis* 53: 81-93.
- Encinar, J.M. Gonzalez, J.F Sabio, E. and Rodríguez, J.J. 2000. Catalyzed gasification of active carbon by oxygen: Influence of catalyst size, temperature, oxygen partial pressure and particle size. *Journal of chemical technology and biotechnology* 75: 213-222.
- Hernandez, M.R. Garcia A.N. Gomez A. Agullo, J. and Marcilla, A. 2006. Effect of residence time on volatile products obtained in the HDPE Pyrolysis in the presence and absence of HZSM-5. *Ing. Eng. Chem. Res.* 45: 8770-8778.
- Jin, Y.Z. Gao, C. Hsu, W.K. Zhu, Y. Huczko, A. Bystrzejewski, M. Roe, M. Lee, C.Y. Acquah, S. Kroto, H. Walton, D.R.M. 2005. Large-scale synthesis and characterization of carbon spheres prepared by direct pyrolysis of hydrocarbons. *Carbon* 43: 1944-1953.
- Marquez-Montesinos, F. Cordero, T. Rodriguez-Mirasol, J. and Rodriguez, J.J. 2002. CO<sub>2</sub> and steam gasification of a grapefruit skin char. *Fuel* 81: 423-429.
- Montgomery, D.C. 1991. *Design and analysis of experiments*. Wiley & Sons, Inc., NY.
- Poustma, M. L. 2003. Reexamination of the pyrolysis of polyethylene: data needs, free radical mechanistic considerations, and thermochemical kinetic simulation of initial product-forming pathways. *Macromolecules* 36: 8931-8957.
- Rodriguez-Mirasol, J. Cordero, T. Rodriguez, J.J. 1997. High-Temperature carbons from kraft lignin. *Carbon* 34: 43-52.